Published in final edited form as:
Nat Commun. 2013 ; 4: 2081. doi:10.1038/ncomms3081.

Thymosin β4-sulfoxide attenuates inflammatory cell infiltration and promotes cardiac wound healing

Mark A. Evans[1], **Nicola Smart**[1], **Karina N. Dubé**[1], **Sveva Bollini**[1], **James E. Clark**[2], **Hayley G. Evans**[3], **Leonie S. Taams**[3], **Rebecca Richardson**[4], **Mathieu Lévesque**[4], **Paul Martin**[4], **Kevin Mills**[5], **Johannes Riegler**[6,7], **Anthony N. Price**[8], **Mark F. Lythgoe**[6], and **Paul R. Riley**[1,*]

[1]Department of Physiology, Anatomy and Genetics, Sherrington Building, University of Oxford, South Parks Road, Oxford, OX1 3PT, UK

[2]Cardiovascular Division, Kings College London, Rayne Institute, St Thomas' Hospital, London, SE1 7EH, UK

[3]Centre for Molecular and Cellular Biology of Inflammation (CMCBI), Division of Immunology, Infection and Inflammatory Disease, King's College London, London SE1 1UL, UK

[4]Department of Biochemistry, Physiology and Pharmacology, University of Bristol, School of Medical Sciences, University Walk, Bristol, BS8 1TD, UK.

[5]UCL-institute of Child Health, London, WC1N 1EH, UK

[6]Centre for Advanced Biomedical Imaging (CABI), Department of Medicine and Institute of Child Health, University College London (UCL), London, WC1E 6DD, UK

[7]Centre for Mathematics and Physics in the Life Sciences and Experimental Biology (CoMPLEX), UCL, London, WC1E 6BT, UK

[8]MRC Clinical Sciences Centre, Faculty of Medicine, Imperial College London, London, W12 0NN, UK

Abstract

The downstream consequences of inflammation in the adult mammalian heart are formation of a non-functional scar, pathological remodelling and heart failure. In zebrafish, hydrogen peroxide (H_2O_2) released from a wound is the initial instructive chemotactic cue for the infiltration of inflammatory cells, however, the identity of a subsequent resolution signal(s), to attenuate chronic inflammation, remains unknown. Here we reveal that Thymosin β4-Sulfoxide inhibits interferon-γ, and increases monocyte dispersal and cell death, lies downstream of H_2O_2 in the wounded fish and triggers depletion of inflammatory macrophages at the injury site. This function is conserved in the mouse and observed after cardiac injury, where it promotes wound healing and reduced scarring. In human T cell/CD14+ monocyte co-cultures, Tβ4-SO inhibits IFN-γ and increases monocyte dispersal and cell death, likely by stimulating superoxide production. Thus, Tβ4-SO is a

[*]To whom correspondence should be addressed: Department of Physiology, Anatomy and Genetics, Sherrington Building, University of Oxford, South Parks Road, Oxford, OX1 3PT Tel. +44 (0) 1865 282366. Fax. +44 (0) 1865 272469. paul.riley@dpag.ox.ac.uk.

AUTHOR CONTRIBUTIONS MAE contributed experiments for MS/MS post-zebrafish tail wounding, mouse MI and ROS assays on spleen monocytes and analysed data. NS contributed data on mouse leukocyte infiltration after MI; KD, SB and JEC performed MI surgeries; HE and LST contributed human monocyte culture data; RR (heart), ML (tail/flank) and PM contributed bead-wounding data and movies in zebrafish; KM performed MS/MS analyses to detect Tβ4-SO in wounded zebrafish larvae; JR, ANP and ML performed MRI to assess scarring and cardiac function in Tβ4-treated mouse hearts. PRR devised the initial hypothesis, supervised experiments and collaborations and wrote manuscript.

CONFLICTS OF INTEREST The authors declare no disclosures or conflicts of interest.

Europe PMC Funders Author Manuscripts

putative target for therapeutic modulation of the immune response, resolution of fibrosis and cardiac repair.

Europe PMC Funders Author Manuscripts

INTRODUCTION

Cardiac injury activates an innate immune mechanism (reviewed in[1]) underpinned by sequential recruitment of inflammatory neutrophils and macrophages (leukocytes) to the site of injury. A direct consequence of immune cell infiltration is activation of fibroblasts and their differentiation to myofibroblasts, the principle source of collagen deposition, fibrosis and scarring. Recently a study in the zebrafish revealed that the earliest "damage" signal that instigates rapid neutrophil and macrophage influx to the wound is hydrogen peroxide (H_2O_2)[2]. The identity of subsequent downstream signalling molecules or cues that encourage the resolution of immune cells away from the wound, once the acute phase is complete, remains unknown[3].

Thymosin β4 (Tβ4) is an actin-binding peptide which exerts both anti-inflammatory and anti-fibrotic effects in the context of tissue wounding; notably following alkali eye injury[4] and blebomyocin-induced damage in the lung[5]. Tβ4 is one of the first proteins to be up-regulated after wounding[6] and has been shown to modulate oxidative stress, targeting cardiac fibroblasts and cardiomyocyte survival following myocardial infarction[7,8]. There are two naturally occurring derivatives of Tβ4, the tetrapeptide Ac-SDKP, an N-terminal cleavage product known to have anti-fibrotic effects during hypertension[9] and which can reverse inflammation and fibrosis in rodents post-MI[10] and Thymosin β4-sulfoxide (Tβ4-SO), formed by oxidation of the methionine-6 residue and thought to be the biologically active, secreted form of the parent peptide. Tβ4-SO is largely unstudied to-date, but has been shown to inhibit neutrophil chemotaxis in vitro and attenuate inflammation in carrageenan-injected mice[11]. We sought to investigate whether Tβ4-SO might act as the immune cell dispersal signal during cardiac wound healing to prevent chronic inflammation.

Here we identify Tβ4-SO as downstream of H_2O_2 acting to disperse inflammatory macrophages and promote healing following tail, body flank or heart injury in zebrafish. This function is conserved in mice, where Tβ4-SO, via a direct effect on leukocytes at key time points within healing myocardium, contributes to reduced fibrosis and scarring in the injured heart. Extrapolating these findings to humans, we show that Tβ4-SO blocks the production of pro-inflammatory IFN-γ to reduce the adhesion of activated monocytes and increases cell death downstream of elevated reactive oxygen species (ROS) production.

RESULTS

Tβ4-SO acts downstream of H_2O_2 in the wounded zebrafish

We initially examined whether mechanical wounding of the zebrafish larval tail fin[2] would lead to production of Tβ4-SO *in-vivo*. The zebrafish has five β-thymosin isoforms arising from successive rounds of gene duplication[12] one of which has been described as the orthologue of Tβ4 (Fig. 1a), however, there are no previous reports describing Tβ4-SO in the zebrafish. Larvae at 72 hours post fertilisation (hpf) were pre-incubated in the presence or absence of the small molecule inhibitor of H_2O_2 diphenyleneiodium (DPI), followed by surgical removal of the tip of the tail fin (Fig. 1b). Levels of Tβ4-SO increased rapidly, one hour post-wounding, by approximately 5-fold from 2.0% +/− 1.4% SEM to 10.4% +/− 1.96% SEM (n=100 wounded tail fins/treatment, n=3 experimental replicates; Student's t-test, $p \leq 0.01$; Fig. 1c). Pre-treatment with DPI resulted in a 3-fold increase (6.4% +/− 0.8% SEM) which was significantly less than that observed in vehicle pre-treated control fish (Student's t-test, $p \leq 0.05$; Fig. 1d). To investigate whether ectopic administration of Tβ4-

SO might directly affect the presence of leukocytes, latex beads pre-adsorbed with synthetic Tβ4-SO, or vehicle control (PBS), were implanted into *Tg[mpo:GFP]* zebrafish (Fig. 1e, f). Bead implantation acted as an injury stimulus resulting in recruitment of L-plastin+ (MPO-) macrophages[13] in the control setting (Fig. 1g). Imaging of fish at 3 and 6 hours, thereafter, indicated a significantly reduced number of macrophages proximal to the Tβ4-SO bead relative to controls (3 hrs: co: 20 +/− 4.65 SEM versus Tβ4-SO: 8.25 +/− 2.39 SEM and 6 hrs: co:17.25 +/− 4.05 SEM versus Tβ4-SO: 8.66 +/− 2.03 SEM (n= mean cell count from 5 bead implanted fish per treatment; Student's t-test, $p \leq 0.01$; Fig. 1h, i), suggesting ectopic Tβ4-SO either inhibited macrophage recruitment or acted to disperse macrophages at the implantation site. MPO+ neutrophil numbers were not significantly affected in this assay; normal neutrophil function involves stimulation of macrophage recruitment (reviewed in[14]), suggesting Tβ4-SO was able to alter macrophage incidence despite the presence of neutrophils. To address the issue of whether Tβ4-SO affected leukocyte recruitment versus dispersal, we generated time lapse movies of the inflammatory cell response in *Tg[LysC:dsRed]*[15] larval zebrafish up to 4 hours following bead implantation. Whilst similar numbers of LysC+ leukocytes were recruited to the bead wound in the control and Tβ4-SO treated setting at 1 and 2 hours post-injury, those that localised to a PBS bead were retained beyond 3 hours post-injury, whereas those that encountered a Tβ4-SO-coated bead dispersed at and beyond this time point, suggesting the latter did not inhibit the initial inflammatory cell recruitment but rather induced their subsequent resolution (Supplementary Fig. S1; Supplementary Movies 1 and 2)

Extrapolating from generic tissue wounding, we next examined the leukocyte response in a model of zebrafish heart injury. Both laser and needle-induced injuries in the larval heart at 72 hours resulted in the release of H_2O_2 from the wound site, as determined by free radical spin trap analysis with 5,5-Dimethyl-1-Pyrroline-N-Oxide (DMPO; Fig. 2a). Delivery of Tβ4-SO or PBS control via microinjection or bathing of the larvae in Tβ4-SO-containing medium, resulted in significantly reduced incidence of infiltrating leukocytes (L-plastin+) at both 3 and 6 hours post-injury (3 hrs: co: 30.4 +/− 2.96 SEM versus Tβ4-SO: 22.5 +/− 1.50 SEM; Student's t-test, $p \leq 0.05$ and 6 hrs: co: 35.3 +/− 3.19 SEM versus Tβ4-SO: 18.2 +/− 1.90 SEM; Student's t-test, $p \leq 0.01$; n= mean cell count from 4 injured fish per treatment; Fig. 2b-f).

Tβ4 and Tβ4-SO reduce inflammatory cell infiltration after MI

To investigate the effect of Tβ4-SO on leukocyte infiltration during wounding in mammals we utilised the mouse MI model. It is known that two distinct phases of monocytes participate post-MI in the mouse: inflammatory monocytes (Ly-6C^{hi}) dominate during the early phase I (days 1-3) and exhibit phagocytic and proteolytic function to digest damaged tissue, whereas monocytes with attenuated inflammatory properties (Ly-6^{lo}) dominate later (from days 4 -7) during the wound healing phase II[16]. Hence, we focused on these key time-points and on the potential for the parent peptide Tβ4 and derivative Tβ4-SO to augment the transition from phase I to II.

We initially treated animals with Tβ4 immediately post-MI and compared against both vehicle-treated controls and Tβ4 global knock-out (equivalent to loss of Tβ4-SO function) mice. MPO+ neutrophils increased in the border zone of the infarct by day 2 and peaked at day 4 post-injury for all mice. Tβ4 treatment attenuated this increase with fewer MPO+ cells present (co: 70 + 14.5 S.E.M versus Tβ4: 30 + 19.1 SEM, $p \leq 0.15$) at the site of injury at both stages (Fig. 3a-d). Global knockout of Tβ4 significantly increased MPO+ cell numbers at the earliest stages of infiltration (day 2; wild type: 20.5 +/− 4.6 SEM versus Tβ4 KO: 47.7 +/− 5.0 SEM; Student's t-test, $p \leq 0.01$), thereafter, numbers were equivalent to that observed for control (vehicle treated) mice (Fig. 3a-d). We next investigated the levels of TNF-α, as the upstream cytokine responsible for initiating the inflammatory cascade[17]. TNF-α was

significantly reduced (6.2-fold reduction) after 2 days of Tβ4 treatment post-MI as compared to vehicle controls (Fig. 3e, f), as was the downstream pro-inflammatory cytokine IL-6 (4.1-fold reduction), which ordinarily is rapidly induced in the ischaemic myocardium (Fig. 3e, f). In keeping with a role in mitigating inflammatory injury during the early stages post-infarct, without interfering with subsequent myocardial healing, Tβ4 stimulated the expression of the inhibitory cytokine IL-10 at 2 days post-MI (8.1-fold increase compared to control; Fig. 3e, f). In control mice the number of F4/80+ macrophages significantly increased between days 2-7 post-MI (Fig. 3g, h, m). Treatment with Tβ4 resulted in an initial increase in F4/80+ cells at day 2 (Fig. 3i, j, m), peaking at day 4 post-MI, followed by a significant reduction at day 7 post-MI (co: 21 +/− 3.4 SEM versus Tβ4: 3 +/− 1.4 SEM; Student's t-test, $p \leq 0.05$; Fig. 3m). In Tβ4 knockout mice we observed the opposite effect, such that F4/80+ cells increased continuously to around 5-fold that of control mice by day 7 post-MI (21 +/− 3.4 SEM versus 135.8 +/− 12.4 SEM; Student's t-test, $p \leq 0.001$; Fig. 3k, l, m). The observation that Tβ4 efficiently cleared the macrophage-rich infiltrate by day 7 post-MI was consistent with the zebrafish data for Tβ4-SO (Fig. 1h, i).

We next investigated the anti-inflammatory activity of Tβ4-SO by flow cytometry of infarct cell suspensions and observed an early (day 2) significant increase in F4/80+ cells (co: 23.0% +/− 2.85% SEM versus Tβ4-SO: 32.0% +/− 2% SEM; n=4; Student's t-test, $p \leq 0.05$; Fig 4a), which represented an increase in the proportion of macrophages, since the total number of monocyte ($CD11b^{hi}$, [Ly6G, B220, CD49b, CD90.2, NK1.1]^{Low}) cells remained unaltered (Fig. 4b). Conversely, 4 days post-injury the total number of monocytes was significantly reduced compared to controls (co: 5.9% +/− 0.95% SEM versus Tβ4-SO: 2.7% +/− 0.4% SEM; n=4; Student's t-test, $p \leq 0.05$; Fig. 4c). Tβ4-SO treatment of infarct suspensions did not, however, alter the relative proportions of monocyte Ly-6^{lo} versus Ly-$6C^{hi}$ sub-populations within the reduced infiltrate at days 2 and 4 post-MI (Supplementary Fig. S2a, b).

These data are consistent with a bi-phasic effect of the influence of Tβ4/Tβ4-SO. During the so-called debris-removal phase 1 (day 2) Tβ4/Tβ4-SO increased macrophage numbers by directing transformation of the stable monocyte pool and subsequently enhanced the transition to the anti-inflammatory phase II (day 4) by signalling monocyte/macrophage clearance from the injury site.

A Tβ4/Tβ4-SO-depleted monocyte infiltrate reduces scarring

The functional consequences of the Tβ4/Tβ4-SO depleted monocyte infiltrate were examined by serial magnetic resonance imaging (MRI) of mice treated with Tβ4, to reflect sulfoxide activity, for 7, 14 and 28 days post-MI. Tβ4-SO was significantly increased in hearts following the addition of Tβ4 across the time course of the study: percentage oxidised Tβ4 increased from 4.7 +/− 1.3% in sham control hearts to 66 +/− 5.1% at day 2 post-MI, maintained at an equivalent elevated level (68.6 +/− 9.3%) through to 28 days post-MI (n=4; repeated measures one-way ANOVA; $p \leq 0.001$). Increase in infarct volume (late gadolinium enhancement; LGE) was significantly higher in PBS compared to Tβ4-treated mice; persisting up to day 28 post-MI (co: 43.3 ± 4.9μl; n=5 versus Tβ4: 22.0 ± 5.3μl; n=4; Student's t-test; $p \leq 0.05$; Fig. 4d) and % infarct relative to left ventricular mass (LVM) followed the same trend (day 28 post-MI: co: 27 ± 2%; n=5 versus Tβ4: 18 ± 4%; n=4; Student's t-test, $p \leq 0.05$; Fig. 4d) indicating that Tβ4/Tβ4-SO reduced infarct size and scarring. The reduced fibrosis was confirmed in the free ventricular wall following Tβ4 treatment (Fig. 4e, f) which, in turn, directly correlated with improved cardiac function as indicated by elevated ejection fraction (EF; Fig. 4g).

Tβ4-SO has anti-inflammatory effects on human monocytes

Extrapolating the animal model findings to human monocytes/macrophages we investigated the response to inflammatory stimuli in the presence of Tβ4-SO. Interactions between CD4+ T-cells and monocyte/macrophages are known to drive pro-inflammatory and anti-inflammatory responses[18]. We established co-cultures of CD4+ T-cells and CD14+ monocytes from the peripheral blood mononuclear cells (PBMC) of healthy individuals and initially excluded any effect of Tβ4 or Tβ4-SO on the underlying T-cells (Supplementary Fig. S3) or the monocyte inflammatory phenotype *per se* via activation or differentiation (Supplementary Fig. S4). The addition of Tβ4-SO lead to a significant reduction in the release of the pro-inflammatory cytokine IFN-γ, relative to controls (co: 1830 pg/ml +/− 365.3 pg/ml SEM versus Tβ4-SO: 1271.5 pg/ml +/− 483.1 SEM, n=4; Wilcoxon matched-pairs signed rank test, p≤0.05; Fig 5a). IFN-γ is secreted by T-cells and functions to both activate macrophages and establish conditions of adhesion and binding required for their migration (reviewed in[19]). CD14+ cells treated with Tβ4-SO were significantly less adherent than their control counterparts, even in the presence of recombinant IFN-γ (co: 219167 +/− 25834 SEM versus Tβ4-SO: 89167 +/− 13411 SEM; n=3; Student's t-test, p≤0.05; Fig. 5b, c). We next assessed whether effects on CD14+ cell adhesion/dispersal might be accompanied by elevated cell death and observed Tβ4-SO significantly increased the number of trypan blue positive cells compared to IFN-γ and control treated cultures (Tβ4-SO: 135833 +/− 22928 SEM versus IFN-γ: 55833 +/− 2203 SEM versus co: 33333 +/− 833 SEM; n=3; p≤0.05; Fig 5d). To determine a potential mechanism, we investigated whether Tβ4-SO, in the presence of IFN-γ, might act to increase intracellular ROS and thus provoke oxidative stress-induced apoptosis[20]. Increased ROS is known to occur downstream of H_2O_2 release and cell survival can be maintained by reversal of H_2O_2-induced oxidation of methionine[21]. Macrophages from the peritoneal cavity of mice were stimulated with IFN-γ and incubated with either vehicle or Tβ4-SO followed by dihydroethidium (DE) a fluorescent indicator of ROS[22]. Activating IFN-γ treatment alone resulted in increased ROS, which was significantly augmented by the addition of Tβ4-SO (n=3; Student's t-test, p≤0.05; Fig. 5e, f); consistent with Tβ4-SO acting downstream of H_2O_2-methionine oxidation and oxidative stress.

DISCUSSION

Despite a number of previous studies assigning anti-inflammatory and anti-fibrotic properties to Tβ4, there remains no insight as to how this peptide might mediate effects directly on the innate immune-cell response post-wounding. Here we sought to test the hypothesis that a naturally occurring oxidised derivative, Tβ4-SO, might act to disperse inflammatory cells from sites of injury in a conserved manner from zebrafish, through rodents, to man. This study was underpinned by prior identification of H_2O_2 as the initial chemo-attractive signal for recruitment of inflammatory cells to a wound[2] and the outstanding question as to what might be the downstream factor responsible for resolving these cells to prevent chronic inflammation[3]. Tβ4-SO is formed by methionine oxidation of Tβ4 in the presence of H_2O_2 which alongside the observed up-regulation of Tβ4 at wound sites[6,23] established the sulfoxide variant as a potential candidate for immune cell dispersal. We initially generated a simple zebrafish tail fin resection model[2] and revealed by QTOF-MS that Tβ4-SO is significantly up-regulated post-wounding in zebrafish in a H_2O_2-dependent manner. In subsequent zebrafish lateral body wall and heart injury models ectopic sulfoxide induced the resolution of leukocytes/macrophages from the site of injury downstream of H_2O_2. Thus, Tβ4-SO may function as the elusive dispersal signal to prevent chronic inflammation and promote wound healing. Extrapolating to mouse MI, both the parent molecule Tβ4 and sulfoxide derivative were necessary and sufficient to ensure an elevated presence of macrophages, within the stable (Ly-6C^{hi}) monocyte pool, during the

debris and necrotic tissue removal phase I, followed by significantly increased clearance during the transition to the wound healing phase II following cardiac injury[16]. These findings collectively suggest Tβ4 through conversion to Tβ4-SO can function to prevent monocytosis and, therefore, excessive granulation tissue formation as an immediate downstream consequence[16]. Functionally, the altered inflammatory infiltrate likely contributes to the reduced fibrosis and scarring, as determined by MRI, and as previously described[16]. However, Tβ4 is also known to promote a range of reparative functions post-MI which will have a significant impact here; including the maintenance of cardiomyocyte survival via Akt signalling[24], the induction of neo-vascularisation and coronary angiogenesis[25,26] and reactivation of adult epicardial cells to contribute to myocardial regeneration[27]. Thus, the anti-inflammatory role described for Tβ4-SO is one of a number of contributory factors reflecting the pleiotropy of Tβ4 in the context of cardiac wound healing and repair. Mechanistically, we observed no effect of either Tβ4/Tβ4-SO on monocyte activation or differentiation, as determined by flow sorting against a signature set of markers (CD16, CD40, HLA-DR, CD54, CD86, CD163, CD206). In human co-cultures the clearance and dispersal was dependent upon a combination of modulating IFN-γ induced cell adhesion, favouring increased human CD14+ monocyte migration, and cell death supported by increased vital dye staining and elevated ROS-mediated apoptosis in murine splenic monocytes. Inflammatory cells are in fact known to release ROS to kill locally invading microbes to prevent infection of wounds[28]; here we introduce the concept of co-opting ROS killing to feedback onto the resolution of the immune cells themselves.

In summary, post-infarction immune cells are required for the transition into a reparative phase, however, their persistence can lead to chronic inflammation, characterised by excessive granulation tissue/scar, attenuated repair and long term pathological remodelling of the injured heart (reviewed in[29,30]). Consequently, timely resolution of the inflammatory infiltrate is essential for optimal infarct healing. Our data are consistent with the Tβ4-SO, formed as a bi-product of H_2O_2 production from the wound site, acting to resolve immune cells and modulate cardiac fibrosis and scarring.

METHODS

MS analysis of Tβ4-SO

72hpf zebrafish were pre-treated for 30 minutes with either 10μM DPI or DMSO followed by resection of the caudal fin. The fish were recovered for 1 hour followed by removal of a small section of tissue immediately proximal to the wound. The tissue was reconstituted in 20μl 100mM Tris, pH 7.8, containing 8M Urea, vortexed for 1 hour, and 1.5μl 0.2M Dithioerythritol (DTE) in 100mM Tris, pH 7.8 was added, vortexed again and the sample incubated at room temperature for 1 hour. 3μl of 0.2M Iodoacetamide in 100mM Tris, pH 7.8 was added, vortexed and incubated for 30minutes at room temperature. Finally, 165μl of H_2O containing 1μg of proteomics grade trypsin (Sigma) was added and incubated for ≥16h at 37°C. Separation of samples and standards was performed using a 2795XE high performance liquid chromatography (HPLC; Waters, UK). The HPLC protocol: isocratic gradient of 95% dH2O: 5% acetonitrile over a 55 min period; flow rate 0.5 ml/min, diverted to waste for the first 1.5 min after sample injection, to minimise accumulation of endogenous compounds on the ionisation source. The HPLC was coupled to a triple quadrupole tandem mass spectrometer (MicroMass Quattro; Waters, UK) operating in negative-ion mode using the following settings: capillary 3.2 kV, source temperature 150 °C, desolvation temperature 350 °C, cone voltage 30 V, cone gas flow rate 90 l/h and desolvation gas flow rate 900 l/h. The MRM mode was used for quantification and data were acquired and processed using MassLynx software (Waters, UK).

In vivo analysis of leukocyte recruitment in zebrafish

Zebrafish were housed and maintained in environmentally controlled aquaria. All surgical and pharmacological procedures were performed in accordance with the Animals (Scientific Procedures) Act 1986 (A(SP)A; Home Office, UK). Wild-type, Tg(mpo:GFP), Tg[LysC:dsRed] or Tg(myl7:GFP) zebrafish larvae (72 hpf) were anaesthetised in MS-222 and placed in 3% methyl cellulose in 0.3% Danieau's solution on a glass slide. Heparin-Ceramic HyperD M Hydrogel Composite beads (Sigma-Aldrich, H0532) were rinsed for 5-10 minutes in 0.3% Danieau's solution five times and pre-soaked in 100 μg/ml Tβ4-SO or PBS for 30 min+ before being inserted through the skin and muscle of the flank region using a fine tungsten needle (World Precision Instruments).

Heart injury was either via microinjection delivery of Tβ4-SO (3 nl of 100 μg/ml) into the heart and pericardial space or implanting of a bead into this region, as described above. Control fish were injected with PBS vehicle or beads soaked in PBS vehicle. For laser injury, fish were pre-treated with 100 μg/ml Tβ4-SO or PBS in Danieau's solution for at least 2 hours, embedded in low-gelling point Agarose (Sigma-Aldrich, A9414) and wounded using a nitrogen ablation laser (Spectra-Physics) attached to a Zeiss Axioplan 2 widefield imaging system. For imaging of H_2O_2 production, 72 hpf Tg(myl7:GFP) larvae were incubated in Danieau's medium containing 200 mM DMPO (Enzo Life Sciences) for five hours, wounded and then sacrificed at 30 mpi. Larvae were fixed in 4% paraformaldehyde overnight at 4 °C and subject to whole-mount immunostaining using rabbit anti-L-plastin (1:500), rabbit anti-DMPO (1:200; ALX-210-530-R050, Enzo Life Sciences) or chicken anti-GFP antibodies (1:200; Invitrogen, A10262). Secondary antibodies: Alexa Fluor 546 or 647 goat anti-rabbit and Alexa Fluor 647 goat anti-chicken (all 1:200; Invitrogen, A11035, A21245, A21449, respectively). Images were taken using a Leica SP5 confocal imaging system attached to a Leica DMI 6000 inverted microscope. For live imaging of LysC:dsRED+ positive leukocyte recruitment to a wound, fish were anaesthetised and a bead inserted as described above. Fish were then embedded in low-gelling point agarose and imaged using the Leica confocal system. Immune cell numbers within a 500 μm radius of the wound site were counted manually using Fiji software.

Myocardial infarction

Mice were housed and maintained in a controlled environment. All surgical and pharmacological procedures were performed in accordance with the Animals (Scientific Procedures) Act 1986 (A(SP)A; Home Office, UK). Myocardial infarction was induced in isoflurane-anaesthetized mice by permanent ligation of the left anterior descending artery (LAD). On recovery, animals received interperitoneal (i.p.) injection of either Tβ4 ($6 mg kg^{-1}$), Tβ4-SO ($6 mg kg^{-1}$) or vehicle (PBS). Further injections were given every second day unless otherwise stated. Hearts were harvested at 2, 4 and 7 days after ligation and either prepared for flow cytometry or immunofluorescence.

Immunofluorescent quantification of cells in MI hearts

Immunofluorescence was performed on hearts post-MI. Hearts were first fixed in 4% paraformaldehyde, mounted in OCT and serially sectioned. Representative sections from the scar region were then stained with the following antibodies: Anti-F4/80, Anti-MPO (Abcam). Images were acquired using a Zeiss AxioImager and cells were counted using the 'cell counter' plugin in Image-J: at least 4 fields of view per section were quantified from ≥3 sections per heart.

Western blotting

Post-MI hearts were lysed in Lamni buffer and proteins resolved on a 2D SDS-PAGE gel. Western blotting was performed using standard methods with antibodies against TNF-α, IL-6, IL-10 (Abcam) and GAPDH (Chemicon). Scanning densitometry was performed and signal quantified using ImageJ.

Flow cytometry

To measure murine macrophages post-MI**,** hearts isolated post-MI were digested into a single cell suspension using 0.1% collagenase type II (Worthington Biochemical) and cells were stained using a standard protocol with the following antibodies (all from BD Biosciences unless stated otherwise): Anti-CD90-APC-Cy7 , 53-2.1, Anti-B220-PE, RA3-6B2, Anti-CD49b-PE, DX5, Anti-NK1.1-PE, PK136, Anti–Ly-6G-PE, 1A8, Anti-CD11b-APC, M1/70, Anti-F4/80-biotin, C1:A3-1 (AbD Serotec), Anti-CD11c-biotin, HL3, Anti-I-A^b-biotin, AF6-120.1, Anti-Ly-6C-FITC, AL-21, Strep-PE-Cy7 was used to label biotinylated antibodies. Monocytes were identified as $CD11b^{hi}$ (CD90/B220/CD49b/NK1.1/Ly-6G)^{lo} (F4/80/I-A^b/CD11c)^{lo} Ly-$6C^{hi/lo}$. Macrophages/dendritic cells were identified as $CD11b^{hi}$ (CD90.2/B220/CD49b/NK1.1/Ly-6G)^{lo} (F4/80/I-A^b/CD11c)^{hi} Ly-$6C^{lo}$. The sub-population percentage was expressed relative to the total number of cells detected by the cytometer unless otherwise stated.

To measure murine peritoneal macrophages, cells were. incubated with IFN-γ (10ng/ml) and Tβ4-SO (100ng/ml) for 16h and then isolated on ice for 30 minutes, followed by centrifugation. Cells were then washed once in PBS and stained using a standard protocol for flow cytometry with the following: Anti–Ly-6G-PE, 1A8 (BD Biosciences), Anti-CD11b-APC, M1/70 (BD Biosciences), DAPI (Sigma), dihydroethidium (DE) (1μm). For FACS experiments with human cells, cells were isolated as above, washed once in PBS, fixed using 2% paraformaldehyde and stained for flow cytometry with the following antibodies: Anti-CD4-PerCP-Cy5.5 (BD Bioscience), Anti-CD14-APC (Serotec), Anti-CD163-FITC (Santa Cruz), Anti-CD206-PE (Immunotec), Anti-CD25-PE (Miltanyi Biotech), Anti-CD28-FITC (Serotec), Anti-CD69-FITC (Serotec) and Anti-Ox40-PE (Biolegend). Anti-CD16 AF488 (Biolegend), Anti-CD14 APC-cy7 (Biolegend), Anti-CD40 PE (Serotech), Anti-HLA-DR PerCP-cy5.5 (BD), Anti-CD86 Pacific Blue (Biolegend), Anti-CD54 AF647 (Biolegend). Murine and human samples were acquired on a BD LSRII equipped with 4 lasers (350, 405, 488, and 633 nm) and BD Canto II analyser, respectively, using FACSDiva and FlowJo software.

MRI analysis

Wild-type C57BL/6J mice treated with Tβ4 or vehicle, were subjected to MRI 7 days after LAD ligation. Where infarct size was within the range of 15–40%, longitudinal studies were performed at 14 and 28 days post-MI. Mice were anaesthetized with isoflurane (4%) and maintained at 37±0.5°C with oxygen and anaesthetics (1–2% isoflurane), supplied via a nose cone (1lmin–1). Cardiorespiratory monitoring and gating were performed using an MR-compatible system (SA Instruments) with needle electrodes inserted into the front limbs and a respiratory pillow placed on the chest. Imaging was performed using a 9.4T VNMRS horizontal bore scanner (Varian) with a shielded gradient system (1,000mTm–1) using a 39mm diameter volume coil (Rapid Biomedical GmbH). An electrocardiogram and respiratory gated spoiled gradient echo sequence was used to acquire cine cardiac images with the following parameters for standard cine acquisitions: Time to echo (TE), 1.18ms; time to repetition (TR), 4.5ms; flip angle, 20°; slice thickness, 1mm; no slice separation, field of view (FOV), 25.6×25.6mm^2; matrix size, 128×128; number of signal averages (NSA), 2. Twenty cine-frames were recorded to cover the cardiac cycle. Infarct size was assessed using late gadolinium enhancement (LGE): 0.6$mmolkg^{-1}$ Gd-DTPA was

administered i.p. followed by a Look-Locker acquisition with multiple time to inversion (TI) to determine the optimum TI, and by a multi-slice inversion recovery (IR) acquisition with flip angle (FA) = 90° using the following imaging parameters: TE, 1.58ms; TR, ~500–600ms; FA, 90°; slice thickness, 0.5mm; 0.5mm slice gap; 7–8 slices; FOV, 25.6×25.6mm^2; matrix size, 192×192; NSA, 2. A second stack of short-axis images offset by 0.5mm was acquired to generate a continuous data set. Randomized and anonymized images were analysed using the cardiac analysis software Segment (http://segment.heiberg.se). To estimate infarct size, endocardial and epicardial borders were segmented on LGE images automatically with manual adjustments followed by automatic delineation of infarct tissue using a built-in fraction of segment. Infarct size, expressed as percentage of left ventricular mass, was calculated as infarct volume/left ventricular volume (from cine data). Comparisons between groups were performed using a repeated measures one-way ANOVA, using R software25 version 2.8.1.

Mouse peritoneal macrophage isolation and assessment of ROS

Adult wild-type C57BL/6J mice were humanely euthanized in accordance with A(SP)A 1986, injected i.p. with 5ml 4°C PBS and then agitated to release macrophages from the peritoneal cavity. The PBS containing the cells was re-isolated and the cells centrifuged at 600g for 10 minutes and washed once with PBS. Cells were then resuspended in RPMI medium 1640 supplemented with 1% penicillin/streptomycin, 1% glutamine, and 10% heat-inactivated FCS and allowed to adhere to the surface of a 24 well plate for 3 hours. Non-adherent (non-macrophage) cells were removed from the well with vigorous washing and macrophages were stimulated with IFN-γ (50ng/ml), PBS supplemented with 100ng/ml Tβ4-SO or PBS alone.

Peripheral Blood Cell Isolation

Ethical approval for the use of peripheral blood from healthy donors was obtained from the Bromley Research Ethics Committee and all subjects provided informed consent. Peripheral blood mononuclear cells were isolated by density gradient centrifugation (lymphocyte separation media; PAA, Pasching, Austria). Purification of cell subsets was performed by magnetic cell sorting (Miltenyi Biotec) and confirmed by flow cytometry. Monocytes (>90% pure) were isolated by positive selection using anti-CD14 microbeads and T-cells also by positive selection using anti-CD4 microbeads (Miltenyi Biotec).

Human Cell Culture

Peripheral blood (PB) was collected from healthy volunteers, following written informed consent. Ethics approval for this study was given by the Bromley Research Ethics Committee (reference 06/Q0705/20). Mononuclear cells were isolated from PB using Ficoll-Hypaque (LSM 1077; PAA Laboratories) density-gradient centrifugation. Bulk $CD4^+$ T cells (1×10^6 per ml) were cultured in 24-well plates in the absence or presence of monocytes in RPMI medium 1640 supplemented with 1% penicillin/streptomycin, 1% glutamine, and 10% heat-inactivated FCS (Cambrex, Nottingham, U.K.) and cultures were stimulated with 100 ng/ml anti-CD3 (OKT3; Ortho Biotech, Bridgewater, NJ). In co-culture 0.5×10^6 monocytes were cultured at a 1:1 ratio with $CD4^+$ T cells for 3 days in 24-well plates. Where indicated, cells were also treated with Tβ4 (100ng/ml), Tβ4-SO (100ng/ml) or PBS.

Quantification of adherence and death of human monocytes

Following 3 days in culture non-adherent and adherent cells were removed separately taking first the media for non-adherent cells and then adding ice-cold PBS prior to detaching the

adherent cells incubated on ice. The number of non-adherent and dead monocytes was then quantified using a trypan blue exclusion assay.

ELISA

Supernatants were collected and analysed for IFN-γ (R&D Systems) and analysed as per the manufacturer's instructions.

Supplementary Material

Refer to Web version on PubMed Central for supplementary material.

Acknowledgments

This work was generously supported by a Medical Research Council grant (reference G0701970).

REFERENCES

1. Frangogiannis NG. The immune system and cardiac repair. Pharmacol.Res. 2008; 58:88–111. [PubMed: 18620057]
2. Niethammer P, Grabher C, Look AT, Mitchison TJ. A tissue-scale gradient of hydrogen peroxide mediates rapid wound detection in zebrafish. Nature. 2009; 459:996–999. [PubMed: 19494811]
3. Martin P, Feng Y. Inflammation: Wound healing in zebrafish. Nature. 2009; 459:921–923. [PubMed: 19536251]
4. Sosne G, et al. Thymosin β 4 promotes corneal wound healing and decreases inflammation in vivo following alkali injury. Exp.Eye Res. 2002; 74:293–299. [PubMed: 11950239]
5. Conte E, et al. Thymosin β4 protects C57BL/6 mice from bleomycin-induced damage in the lung. European journal of clinical investigation. 2013; 43:309–315. [PubMed: 23320620]
6. Malinda KM, et al. Thymosin β4 accelerates wound healing. J.Invest Dermatol. 1999; 113:364–368. [PubMed: 10469335]
7. Kumar S, Gupta S. Thymosin β 4 prevents oxidative stress by targeting antioxidant and anti-apoptotic genes in cardiac fibroblasts. PloS one. 2011; 6:e26912. [PubMed: 22046407]
8. Gupta S, et al. Thymosin β4 and cardiac protection: implication in inflammation and fibrosis. Annals of the New York Academy of Sciences. 2012; 1269:84–91. [PubMed: 23045975]
9. Rasoul S, et al. Antifibrotic effect of Ac-SDKP and angiotensin-converting enzyme inhibition in hypertension. J.Hypertens. 2004; 22:593–603. [PubMed: 15076166]
10. Yang F, et al. Ac-SDKP reverses inflammation and fibrosis in rats with heart failure after myocardial infarction. Hypertension. 2004; 43:229–236. [PubMed: 14691195]
11. Young JD, et al. Thymosin β 4 sulfoxide is an anti-inflammatory agent generated by monocytes in the presence of glucocorticoids. Nat.Med. 1999; 5:1424–1427. [PubMed: 10581087]
12. Edwards J. Vertebrate β-thymosins: conserved synteny reveals the relationship between those of bony fish and of land vertebrates. FEBS Lett. 2010; 584:1047–1053. [PubMed: 20138884]
13. Feng Y, Santoriello C, Mione M, Hurlstone A, Martin P. Live imaging of innate immune cell sensing of transformed cells in zebrafish larvae: parallels between tumor initiation and wound inflammation. PLoS biology. 2010; 8:e1000562. [PubMed: 21179501]
14. Soehnlein O, Lindbom L. Phagocyte partnership during the onset and resolution of inflammation. Nat.Rev.Immunol. 2010; 10:427–439. [PubMed: 20498669]
15. Hall C, Flores MV, Storm T, Crosier K, Crosier P. The zebrafish lysozyme C promoter drives myeloid-specific expression in transgenic fish. BMC developmental biology. 2007; 7:42. doi: 10.1186/1471-213X-7-42. [PubMed: 17477879]
16. Nahrendorf M, et al. The healing myocardium sequentially mobilizes two monocyte subsets with divergent and complementary functions. J.Exp.Med. 2007; 204:3037–3047. [PubMed: 18025128]

17. Frangogiannis NG, et al. Resident cardiac mast cells degranulate and release preformed TNF-alpha, initiating the cytokine cascade in experimental canine myocardial ischemia/reperfusion. Circulation. 1998; 98:699–710. [PubMed: 9715863]
18. Taams LS, et al. Modulation of monocyte/macrophage function by human CD4+CD25+ regulatory T cells. Hum.Immunol. 2005; 66:222–230. [PubMed: 15784460]
19. Schroder K, Hertzog PJ, Ravasi T, Hume DA. Interferon-gamma: an overview of signals, mechanisms and functions. J.Leukoc.Biol. 2004; 75:163–189. [PubMed: 14525967]
20. Simon HU, Haj-Yehia A, Levi-Schaffer F. Role of reactive oxygen species (ROS) in apoptosis induction. Apoptosis. 2000; 5:415–418. [PubMed: 11256882]
21. Yermolaieva O, et al. Methionine sulfoxide reductase A protects neuronal cells against brief hypoxia/reoxygenation. Proc.Natl.Acad.Sci.U.S.A. 2004; 101:1159–1164. [PubMed: 14745014]
22. Rothe G, Valet G. Flow cytometric analysis of respiratory burst activity in phagocytes with hydroethidine and 2′,7′-dichlorofluorescin. J.Leukoc.Biol. 1990; 47:440–448. [PubMed: 2159514]
23. Smart N, et al. Thymosin β4 induces adult epicardial progenitor mobilization and neovascularization. Nature. 2007; 445:177–182. [PubMed: 17108969]
24. Bock-Marquette I, Saxena A, White MD, Dimaio JM, Srivastava D. Thymosin β4 activates integrin-linked kinase and promotes cardiac cell migration, survival and cardiac repair. Nature. 2004; 432:466–472. [PubMed: 15565145]
25. Bock-Marquette I, et al. Thymosin β4 mediated PKC activation is essential to initiate the embryonic coronary developmental program and epicardial progenitor cell activation in adult mice in vivo. J.Mol.Cell Cardiol. 2009; 46:728–738. [PubMed: 19358334]
26. Smart N, et al. Thymosin á4 facilitates epicardial neovascularization of the injured adult heart. Ann.N.Y.Acad.Sci. 2010; 1194:97–104. [PubMed: 20536455]
27. Smart N, et al. De novo cardiomyocytes from within the activated adult heart after injury. Nature. 2011; 474:640–644. [PubMed: 21654746]
28. Schafer M, Werner S. Oxidative stress in normal and impaired wound repair. Pharmacological research : the official journal of the Italian Pharmacological Society. 2008; 58:165–171. [PubMed: 18617006]
29. Frangogiannis NG, Smith CW, Entman ML. The inflammatory response in myocardial infarction. Cardiovasc.Res. 2002; 53:31–47. [PubMed: 11744011]
30. Aoki S, et al. Elevated peripheral blood mononuclear cell count is an independent predictor of left ventricular remodeling in patients with acute myocardial infarction. J.Cardiol. 2011; 57:202–207. [PubMed: 21168993]

Europe PMC Funders Author Manuscripts

Europe PMC Funders Author Manuscripts

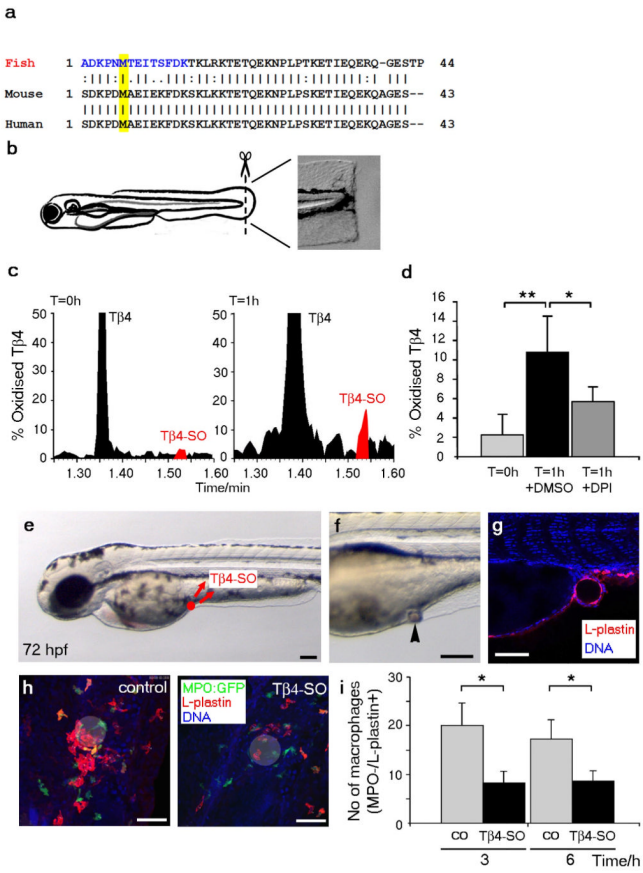

Figure 1. Tβ4-SO acts downstream of H_2O_2 and reduces macrophage accumulation in zebrafish wounds

Alignment of Tβ4 orthologues: highlighted in blue is the predicted trypsin-digest peptide fragment of the fish sequence for MS and in yellow the conserved methionine at position 6 (**a**). Schematic of the tail fin injury model at 72 hours post-fertilisation (hpf) and an example of a tail fin post-wounding (**b**). Individual spectra from QTOF-MS of wounded tail fin samples, at time zero and 1 hour post-wounding, confirming detection and increase over time of parent Tβ4 and oxidised derivative Tβ4-SO (**c**). Quantification revealed a significant elevation in Tβ4-SO in wounded tissue after 1 hour which was abrogated by prior incubation with the H_2O_2 inhibitor diphenyleneiodium (DPI; n=5 fish per treatment, error bars are standard error of the mean (SEM; **d**). Zebrafish larva at 72 hr, indicating site of implantation of Tβ4-SO-soaked bead (**e**) and an actual bead in the lateral body wall (**f**). Bead implantation acted as a wound, as demonstrated by infiltration of L-plastin+ leukocytes (**g**). Immunostaining of fish 6 hours post-bead implantation revealed significant presence of neutrophils (MPO:GFP+), and macrophages (MPO-/L-plastin+) proximal to a control (vehicle-soaked) bead compared to a Tβ4-SO bead (**h**). Quantification of neutrophils and macrophages within a 500 μm radius of the bead wound site, revealed a significant reduction of MPO-/L-plastin+ macrophages proximal to Tβ4-SO beads as compared to controls at 3 and 6 hours; n=5 fish per treatment, error bars are standard error of the mean (SEM; (**i**)). Scale bars: **e** represents 100 μm; **f**, 100 μm; **g**, 150 μm; **h**, 20 μm. All statistics Student's t-test; * $p \leq 0.05$, ** $p \leq 0.01$.

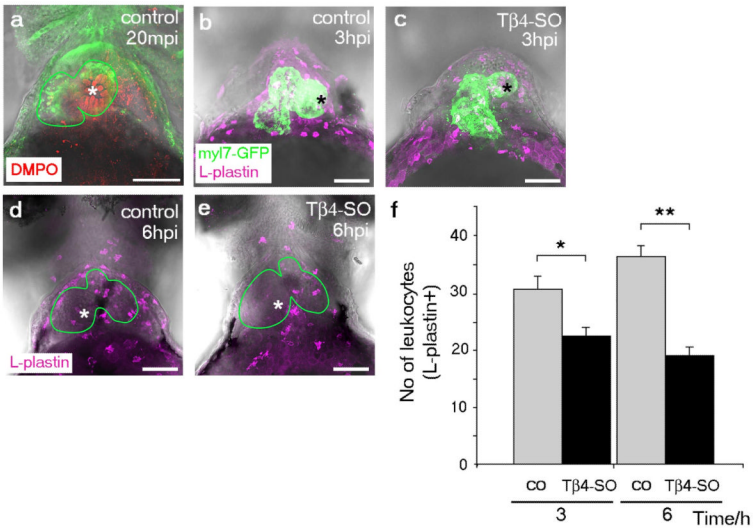

Figure 2. Tβ4-SO disperses leukocytes after cardiac injury in zebrafish

(**a**). Laser injury to the heart of a 72 hr zebrafish larvae immunostained for 5,5-Dimethyl-l-Pyrroline-N-Oxide (DMPO; red) revealed localised H_2O_2 production at the wound site (**b**). At 3 hours post laser heart injury (hpi), a reduced leukocytic response (revealed by L-plastin staining – magenta; **c**, **d**) was seen in Tβ4-SO treated fish within 500 μm of the focal point of injury (**c**) compared to controls (**b**). Larger, needle-induced wounds to the heart region of *Tg[myl7:GFP]* transgenic fish, resulted in a stronger inflammatory response in PBS-treated control hearts at 6 hpi (**d**), which was significantly reduced in Tβ4-SO treated fish (**e**). Total numbers of L-plastin+ leukocytes was significantly lower at 3 and 6 hpi for Tβ4-SO treated fish compared to controls; n=5 fish per treatment, error bars are standard error of the mean (SEM) (**f**). Asterisks mark wound site and green outlines delineate the heart as determined by myl7-GFP+. Scale bars: **a**-**e**, 100 μm. All statistics Student's t-test; * $p \leq 0.05$, ** $p \leq 0.01$.

Europe PMC Funders Author Manuscripts

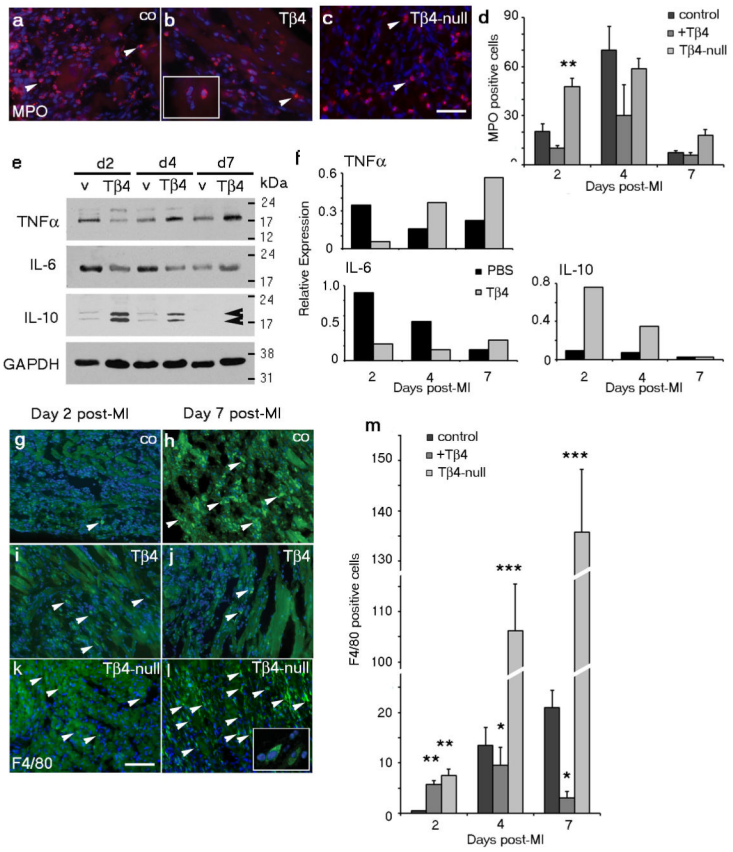

Figure 3. Tβ4/Tβ4-SO modulates the inflammatory response post-MI in the mouse heart

Representative images, showing infiltration of the injured myocardium with neutrophils (white arrowheads highlight individual MPO+ cells; **a-c**) and macrophages (white arrowheads highlight individual F4/80 cells; **g-l**) in Tβ4-treated, control vehicle-treated and Tβ4-null myocardial infarction (MI) hearts. Significantly fewer cytotoxic myeloperoxidase (MPO)-peroxidase+ neutrophils were present in Tβ4-treated, compared with controls and Tβ4-null hearts at days 2 and 4 post-MI (**a-d**). Inset in (**b**) illustrates specific MPO staining of a neutrophil at higher magnification. Significantly more neutrophils were present at the infarct site in the Tβ4-null hearts at day 2, consistent with the timing of initial inflammatory cell infiltration (**d**). Western blots for TNF-α, IL-6, IL-10 and GAPDH at 2, 4 and 7 days post-MI in animals treated with Tβ4 as compared to vehicle controls (**e**) and quantification of protein expression by scanning densitometry (**f**). Black arrowheads indicate alternate glycosylated isoforms (21kDa and 24kDa) of IL-10. The upstream initiator of the acute inflammatory cascade, TNF-α, is down-regulated at early stages post-MI (2 days) following Tβ4 treatment along with the downstream inflammatory cytokine, IL-6; levels of both TNFα and IL-6 subsequently become elevated after 7 days consistent with an early reduction in injury and enhanced repair at later stages (**e, f**). The anti-inflammatory cytokine IL-10 is up-regulated after 2 and 4 days of treatment with Tβ4 (**e, f**). Representative images, F4/80 positive macrophages in the scar region post-MI, in co (**g, h**), Tβ4 treated (**i, j**) or $T\beta4^{-/-}$ animals (**k, l**); both at day 2 (**g, i, k**) and day 7 (**h, j, l**) post-MI, with cell counts quantified in (**m**). Tβ4-induced macrophage infiltration peaks at day 4 but is rapidly cleared, to a level significantly reduced relative to vehicle-treated by day 7; in Tβ4-null hearts the incidence of macrophages at the wound was significantly elevated relative to the controls as highlighted by cell counts (**m**). Scale bar: **c** represents 20 μm (applies to **a-c**) and K represents 20 μm (applies to **g-l**); v, vehicle; n=4-6 MI hearts analysed per time point; error bars are standard

error of the mean for all bar graphs; all statistics Student's t-test; * $p \leq 0.05$, ** $p \leq 0.01$, ***$p \leq 0.001$.

Europe PMC Funders Author Manuscripts

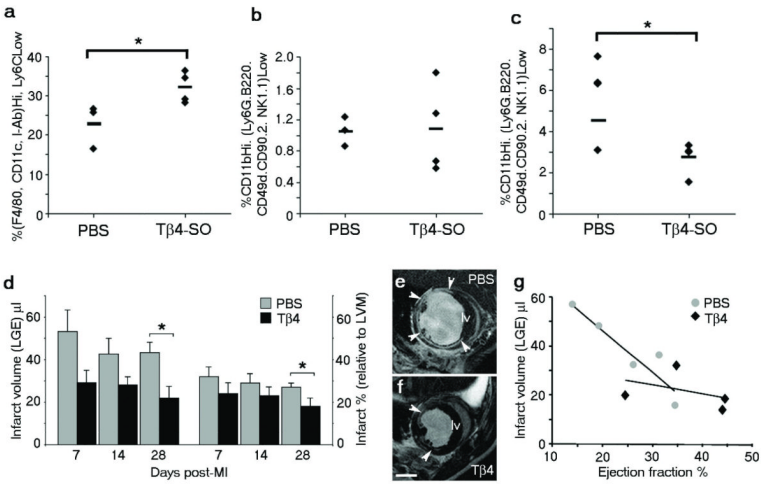

Figure 4. Tβ4/Tβ4-SO attenuates inflammatory cell infiltration, scarring and fibrosis

Following treatment with Tβ4-SO, FACS analyses at 2 days post-MI revealed a significant increase in macrophages at day 2 post-MI (**a**), with no change in the total number of monocytes recruited (**b**). In MI samples 4 days post injury the total number of monocytes was significantly reduced (**c**). Tβ4 treatment resulted in significantly increased Tβ4-SO levels (refer to main text) and reduced scarring and fibrosis, by 28 days post-MI, according to surrogate measures of infarct volume and % infarct relative to left ventricular mass (LVM); as determined by longitudinal MRI of late gadolinium enhancement (LGE); n=4 hearts per treatment per time point; error bars are standard error of the mean (SEM; **d**). Short axis MRI images of PBS control (**e**) and Tβ4 (**f**) treated hearts at day 28 post-MI highlighted the extent of infarct and fibrosis (white arrowheads) in the wall of the left ventricle (lv) which is reduced in Tβ4 treated animals (comparing **e** with **f**). Infarct volume negatively correlated with ejection fraction at day 28 MI, consistent with the late remodelling phase and reduced LGE in Tβ4 treated hearts (slope: -0.37; p=0.624) compared to PBS controls (slope: -1.76; p=0.0234) reflected reduced scar formation (**g**). Scale bars: **f** represents 2mm; Statistics repeated measures one-way ANOVA; *p ≤0.05.

Europe PMC Funders Author Manuscripts

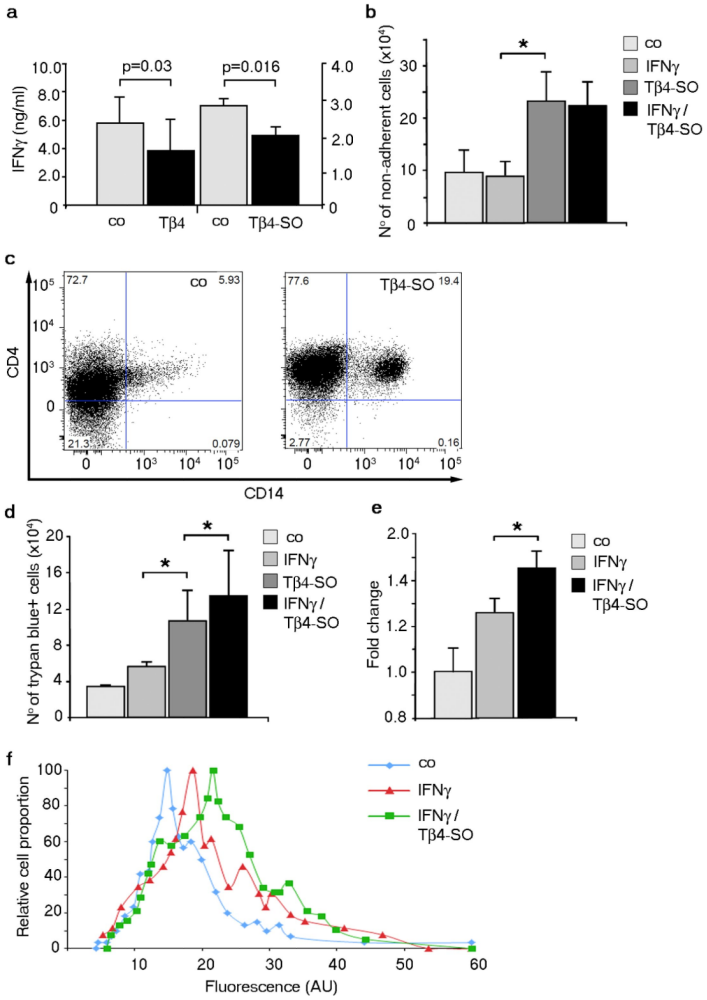

Figure 5. Tβ4-SO reduces adhesion and increases cell death of human monocytes via increased ROS

Co-cultures of human CD14+ monocytes and CD4+ T-cells treated with either Tβ4 or Tβ4-SO resulted in significantly decreased levels of IFNγ; n=4 co-cultures per treatment; error bars are standard error of the mean (SEM; **a**). In both single CD14+ monocyte cultures and co-cultures with CD4+ T-cells, Tβ4-SO significantly reduced the adherence of the cells in the presence of IFNγ; n=3 cultures per treatment; error bars are standard error of the mean (SEM; **b, c**); presence of cells in the right FACS quadrant reflects non-adherent monocytes when treated with Tβ4-SO (**c**). Vital dye staining (trypan blue) of CD14+ cultures demonstrated Tβ4-SO significantly increased monocyte cell death, which was further increased by the additive effect of IFNγ; n=3 cultures per treatment; error bars are standard error of the mean (SEM; **d**). In isolated murine peritoneal macrophages Tβ4-SO resulted in a significant fold increase in reactive oxygen species (ROS); n=3 cultures per treatment; error bars are standard error of the mean (SEM; **e**) which was reflected by increased dihydroethidium (DE) fluorescence (**f**). Statistics: Wilcoxon matched-pairs signed rank test (**a**) and Student's t-test (**b**, **d**, **e**); * $p \leq 0.05$.